Published online 15 February 2010 *Nucleic Acids Research, 2010, Vol. 38, No. 11* ***3533–3545***
doi:10.1093/nar/gkq076

Histone H1 null vertebrate cells exhibit altered nucleosome architecture

Hideharu Hashimoto[1,2], Yasunari Takami[3], Eiichiro Sonoda[4], Tomohito Iwasaki[5], Hidetomo Iwano[6], Makoto Tachibana[1,2], Shunichi Takeda[4], Tatsuo Nakayama[3,7], Hiroshi Kimura[8] and Yoichi Shinkai[1,2,*]

[1]Experimental Research Center for Infectious Diseases, Institute for Virus Research, Kyoto University, Shogoin Kawara-cho, [2]Department of Molecular and Cellular Biology, Graduate School of Biostudies, Kyoto University, Shogoin Kawara-cho, Kyoto 606-8507, [3]Section of Biochemistry and Molecular Biology, Department of Medical Sciences, Miyazaki Medical College, University of Miyazaki, 5200 Kihara, Kiyotake, Miyazaki 889-1692, [4]Department of Radiation Genetics, Faculty of Medicine, Kyoto University, Yoshida Konoe, Kyoto, 606-8315, [5]Department of Food Science, Rakuno Gakuen University, Ebetsu, [6]Department of Veterinary Biochemistry, Graduate School of Veterinary Medicine, Rakuno Gakuen University, Ebetsu, Hokkaido 069-8501, [7]Department of Life Science, Frontier Science Research Center, University of Miyazaki, 5200 Kihara, Kiyotake, Miyazaki 889-1692 and [8]Graduate School of Frontier Bioscience, Osaka University, Suita, Osaka 565-0871, Japan

Received February 21, 2009; Revised January 19, 2010; Accepted January 26, 2010

ABSTRACT

In eukaryotic nuclei, DNA is wrapped around an octamer of core histones to form nucleosomes, and chromatin fibers are thought to be stabilized by linker histones of the H1 type. Higher eukaryotes express multiple variants of histone H1; chickens possess six H1 variants. Here, we generated and analyzed the phenotype of a complete deletion of histone H1 genes in chicken cells. The H1-null cells showed decreased global nucleosome spacing, expanded nuclear volumes, and increased chromosome aberration rates, although proper mitotic chromatin structure appeared to be maintained. Expression array analysis revealed that the transcription of multiple genes was affected and was mostly downregulated in histone H1-deficient cells. This report describes the first histone H1 complete knockout cells in vertebrates and suggests that linker histone H1, while not required for mitotic chromatin condensation, plays important roles in nucleosome spacing and interphase chromatin compaction and acts as a global transcription regulator.

INTRODUCTION

The fundamental unit of chromatin is the nucleosome, which comprises an octamer of core histones, H2A, H2B, H3 and H4, wrapped around 146 or 147 bp of DNA (1,2). The linker histone H1 binds to the core particles and protects an additional ~20 bp of DNA (linker DNA). Several lines of evidence suggest that H1 plays an important role in establishing and maintaining the structure of the chromatin fiber (3–5). However, linker histone H1 is not evolutionarily conserved as extensively as other core histones (6). In higher eukaryotes, histone H1 consists of a globular domain with N-terminal and C-terminal tails, but this domain structure is not conserved in unicellular organisms. Macronuclear histone H1 of *Tetrahymena* only has a C-terminal tail, and *Saccharomyces cerevisiae* Hho1 has two globular domains. In unicellular organisms such as *Tetrahymena thermophila*, *S. cerevisiae* and *Aspergillus nidulans*, depletion of histone H1 or the H1-like protein does not induce global transcriptional upregulation, but instead affects only a small subset of genes, resulting in little effect on cell growth and chromatin condensation and segregation (7–10). *Tetrahymena* strains deficient in *HHO* (encoding macronuclear histone H1) and *MLH* (encoding micronuclear linker histone) exhibit enlarged macro- and

*To whom correspondence should be addressed. Tel: +81 75 751 3990; Fax: +81 75 751 3991; Email: yshinkai@virus.kyoto-u.ac.jp
Present address:
Hideharu Hashimoto, Department of Biochemistry, Emory University, 1510 Clifton Rd Atlanta, GA 30322, USA.

The authors wish it to be known that, in their opinion, the last two authors should be regarded as joint Last Authors.

© The Author(s) 2010. Published by Oxford University Press.
This is an Open Access article distributed under the terms of the Creative Commons Attribution Non-Commercial License (http://creativecommons.org/licenses/by-nc/2.5), which permits unrestricted non-commercial use, distribution, and reproduction in any medium, provided the original work is properly cited.

micro-nuclei, respectively, and the micronuclear mitotic chromosome structure is slightly less condensed in *MLH*-deficient cells (8).

Among higher eukaryotes, the domain structure of histone H1 is conserved, but multiple variants (six for chickens and eight for mice) exist (11,12). So far, knockout (KO) phenotypes of single and multiple histone H1 variants have been reported (4,13–17). Single histone H1 variant KO studies show that none of the histone H1 variants appears to be essential for cell growth and that the expression of only a subset of genes is affected. However, triple *H1* (*H1c, H1d* and *H1e*) KO mice are embryonic lethal (4). Phenotypes generated in knockdown studies in mammalian cell lines are slightly different from those in KO studies, showing that mouse H1.2 and H1.4 are involved in cell cycle and cell death (18). Knockdown of *H1* in *Drosophila* also induces embryonic lethality, suggesting that H1 is generally important in embryogenesis (4,19).

To further elucidate the role of linker histone H1 in higher eukaryotes, particularly under nonredundant conditions, we established completely histone H1-deficient mutant cells using the chicken B lymphocyte line DT40. Herein we describe the phenotype of histone H1-null mutant cells and discuss the potential role(s) of histone H1 in stabilizing chromatin structure, growth rate and chromosomal aberrations, in addition to its function as a global transcription regulator.

MATERIALS AND METHODS

Cell lines, cell culture and plasmid construction

Generation of $H1^{\Delta 10/12}$ H1-DT40 cells (clone name: 17-3-41-25) and $H1^{\Delta 11/12}$ DT40 cells (clone name: 17-3-41-25-13) has been previously described (13). Cells were cultured in RPMI 1640 medium supplemented with 10 μM 2-mercaptoethanol, 10% fetal calf serum (FCS) (Gibco) and 1% chicken serum (Gibco) at 39.5°C. DNA transfection was carried out as previously described (20). Briefly, for each transfection, 1×10^7 cells were suspended in 0.5 ml phosphate-buffered saline (PBS) containing 25 μg of linearized plasmid and electroporated with a Gene Pulser apparatus (BioRad) at 550 V and 25 μF. Following electroporation, cells were transferred into 20 ml of fresh medium and incubated for 24 h. Cells were then divided into four 96-well microtiter plates (0.2 ml/well) and selected with either 0.25 μg/ml Zeocin or 0.5 μg/ml puromycin. To generate the bleomycin-resistant targeting construct, *pΔ02H1/Bleo*, the DNA fragment with the bleomycin-resistant gene driven by the beta-actin promoter was subcloned into the BclI site of the plasmid containing the *02H1* gene (*02H1* ORF) and linearized by BamHI. The floxed C-terminal-enhanced green fluorescence protein (eGFP) fusion histone H1R variant *H1R-eGFP* expression vector, Flox2-*H1R-eGFP-IRES-puro*, was generated as follows. The BglII/NotI fragment of *H1R-eGFP* (20) was subcloned into the pCAGGS-IRES-puromycin-expressing vector (a kind gift from Hitoshi Niwa at RIKEN), and loxP sequences were introduced into the 5′ region of the ATG start site and the 3′ region of the polyA sequences. The floxed *H1R-eGFP* expression vector was linearized by AhdI. The Mer-Cre-Mer expression vector (a kind gift from Michael Reth) was linearized by ScaI. The genome-integrated floxed *H1R-eGFP* transgene in $H1^{\Delta 12/12+\mathrm{flox}}$ (clone name: K11) was deleted by treatment with 4-OHT (100 nM) for 5 days.

Southern blot analysis

Southern blotting was performed as previously described (13,17,20).

Flow cytometry analysis

For cell cycle analyses, cells were labeled for 10 min with 20 μM bromodeoxyuridine (BrdU) (Amersham). They were then harvested and fixed at 4°C overnight with 70% ethanol and successively incubated as follows: (i) in 4N HCl, 0.5% Triton X-100 for 30 min at room temperature; (ii) with FITC-conjugated anti-BrdU antibody (Pharmingen, San Diego, CA, USA) for 1 h at room temperature; and (iii) in 5 μg/ml propidium iodide (PI) in PBS. Between each incubation, cells were washed with PBS containing 5% FCS and 0.1% sodium azide. Subsequent flow cytometric analysis was performed on a FACScan (Becton Dickinson, Mountain View, CA, USA). Fluorescence data were displayed as dot plots using the Cell Quest software (Becton Dickinson).

For measurement of mitotic index, cells exposed to 2.3 Gy IR or unirradiated cells were cultured in the presence or absence of colcemid (0.1 μg/ml), and the cells were collected at 1-h intervals. The fraction of mitotic cells was measured by flow cytometry using an antibody directed against histone H3 serine 10 phosphorylation (H3S10ph) as follows. Cells were washed in PBS once, fixed in 3.5% formaldehyde containing PBS for 10 min at 37°C, and refixed in 90% methanol for 30 min on ice. The fixed cells were washed in incubation buffer (0.5 mg/ml of BSA containing 1× PBS) twice, and incubated with rabbit anti-phospho-histone H3 Serine 10 antibody (1:100; Cell Signaling) in incubation buffer for 30 min. Cells were then incubated with FITC-conjugated anti-rabbit IgG (1:100; Santa Cruz) for 30 min. Cells were finally stained with 1 μg/ml of PI and treated with 10 μg/ml of RNase A.

Nuclear volume measurement

Cells were fixed with 4% paraformaldehyde and stained with 6-diamino-2-phenylindole (DAPI), and *z*-stack images were collected at 1-μm intervals using a FV-1000 confocal microscope (Olympus). The nuclear area in each section was measured using ImageJ software (NIH), and the total nuclear volume was obtained by summing the area of all sections showing DAPI signal. At least 27 interphase nuclei were analyzed in each cell line.

Cell growth assay

Cells were passed every 3 or 4 days ($2.5–5 \times 10^3$ cells/ml for wild-type or $5–10 \times 10^3$ cells/ml for H1 mutant cells) and the total number of cells were counted at each passing time. For a growth competition assay, $H1^{\Delta 11/12+\mathrm{flox}}$ and

$H1^{\Delta 12/12+flox}$ cells were cultured in the presence or absence of OHT for 4 days. Then, the treated and untreated cells were mixed in a 10:1 ratio and monitored for GFP positive (H1R-eGFP depleted) population by flow cytometric analysis.

Detection of chromosomal aberration

Measurement of chromosomal aberration was performed as previously described (20,21). Briefly, 5 ml of a 2×10^5 cells/ml suspension was treated with 0.1 μg/ml of colcemid for 1.5 h prior to analysis. Cells were subsequently harvested and then incubated in 1 ml of 0.9% sodium citrate for 15 min after which 4 ml of Carnoy's solution (methanol:acetic acid = 3:1) was added. After centrifugation for 5 min (150 *g*), cells were further incubated in 5 ml of Carnoy's solution for 30 min at room temperature. Cells were centrifuged again for 5 min (150 *g*), resuspended in 200 μl of fresh Carnoy's solution, and dropped onto glass slides prewetted with 50% ethanol. After drying overnight, slides were immersed into 3% Giemsa solution diluted in 50 mM phosphate buffer (pH 6.4) for 10 min, washed with tap water, completely dried at room temperature, and mounted with Entellan® New. Genomic aberrations were counted (11 macro-chromosomes and Z-chromosomes/sample) following the criteria of ISCN. Aberration examples are shown in Supplementary Figure S2. Chromosomes were analyzed using a Zeiss AxioPhoto microscope (100 × objective lens).

Preparation of acid-extracted histones

Cells ($4–5 \times 10^7$) were washed once with 1 × PBS(–) and suspended in 1 ml of HM buffer [10 mM HEPES (pH 7.0), 2 mM $MgCl_2$], containing 0.2% Triton-X100. Nuclei were collected by centrifugation at 3000 r.p.m. for 5 min and washed with HM buffer. Then, nuclei were washed with HM buffer containing 150 mM NaCl, and collected by centrifugation at 15 000 r.p.m. for 5 min. Nuclei were resuspended with 0.2 M H_2SO_4 and incubated for 1 h at 4°C to extract the histone fraction. After centrifugation at 15 000 r.p.m. for 15 min, the supernatant was collected and divided into two tubes. To prepare the H_2SO_4 histone extract, trichloroacetic acid (TCA) was added to one tube at a final concentration of 20%. To prepare $HClO_4$ histone H1 extract, perchloric acid was added to another tube at a final concentration of 5% and incubated for 1 h on ice before the addition of TCA. After further incubation on ice for 1 h, the tubes were centrifuged, and the precipitates thus obtained were washed with acetone–HCl and twice with acetone before being suspended in 40–50 μl of 8 M Urea – 1 × SDS buffer (13,23).

Western blot analysis

The relative levels of HMG1 and HMG2 proteins in total cell lysate and chromatin fraction were estimated among wild-type and H1 mutant DT40 cells by western blot analysis. Chromatin-bound fraction was prepared by treating cells with 0.2% Triton-X 100 followed by extraction with 0.2 M H_2SO_4, as described above. Different amounts of protein samples ($0.5–4 \times 10^5$ cell equivalent/lane) were separated by SDS-PAGE before western blotting using anti-HMG1/2 monoclonal antibody (clone FBH7; 1:2000), which cross-reacts with both chicken HMG1 and HMG2 (23). H1R-eGFP was detected using anti-GFP (MBL; 1:1000).

MNase digestion and NRL measurement

Nuclear preparation for MNase digestion was performed as described previously (4). Cells were harvested, washed with PBS(–), and suspended in 0.5% NP-40 in RSB [10 mM Tris–Cl (7.5), 10 mM NaCl, 1 mM $CaCl_2$, 3 mM $MgCl_2$ and 0.5 mM phenylmethylsulfonyl fluoride] (2×10^7/ml) for 20 min on ice. Then, the cells were homogenized with 15 strokes of pestle A in a Dounce homogenizer, centrifuged for 6 min at 1000 *g*, and the nuclear pellets were resuspended in RSB (2×10^7/100 μl). Nuclei were digested with MNase (Takara) for 5 min at 37°C (0.05 and 0.4 U MNase for 4×10^6 nuclei/20 μl). Reactions were terminated by addition of 5 mM ethylene-diamine-tetra-acetic acid. Then, chromatin was treated with proteinase K (100 μg/ml) for 90 min at 56°C, extracted with phenol–chloroform, precipitated with alcohol in the presence of 0.3 M Na-acetate, and the pellet was resuspended in TE buffer containing RNase. NRL measurement was done in 1% agarose gel in Tris acetate buffer. DNA sizes of different nucleosome units were calculated from their gel migration distance using the following formula: [DNA length] $= A \times e^{-B \times [\text{mobility}]} + C$ (where the values of A, B and C were obtained by fitting to a curve obtained using 100-bp ladder standards). Then NRL was calculated using the following formula: [DNA size] = [NRL] × [number of nucleosome] + D (where D is a variable number). The mean square displacement, r^2, ranged between 0.9989 and 0.9995. All fitting analyses were done using PRISM 5 (GraphPad Software, Inc.).

Expression array analysis

Exponentially growing DT40 cells cultured in medium containing 100 nM Z-VAD-FMK were harvested, and total RNA was prepared using Sepasol RNA-I (Nakalai Tesque, Kyoto, Japan) following the manufacturer's instructions and further purified with RNeasy (QIAGEN). Purified total RNA (5 μg) was used to synthesize cRNA with a one-cycle labeling kit (Affymetrix) according to the manufacturer's instructions. cRNAs were hybridized to a chicken genome array (Affymetrix). Fluorescent intensities were measured with a GeneChip Scanner 3000 and analyzed with GeneChip Operating Software v3.5 (Affymetrix); data were further analyzed with GeneSpring GX v7.2 (Agilent Technologies). Duplicated array hybridizations were performed for cRNAs from $H1^{\Delta 12/f2+flox}$ (clone name: K11), $H1^{\Delta 12/12}$ #1 (clone name: K11-5) and wild-type DT40 cells. Duplicate expression array data were deposited with the NIH Gene Expression Omnibus (http://www.ncbi.nlm.nih.gov/projects/geo/: accession number GSE8483). Each raw data point was normalized to 1.000 per chip. Probes other than absent-tagged probes, with a raw signal of less than 100.0 among all three genotypes, were rejected.

Probes showing more than two sigma difference between two duplicate chips were also rejected. Then, we excluded selectable marker gene probes and internal control probes. The total number of probes used was 7442 probes per chip.

RESULTS

Generation of histone H1-null DT40 mutant cells

The chicken genome encodes six histone H1 variants (a total of 12 *H1* alleles). We previously established a DT40 mutant cell line, $H1^{\Delta 11/12}$ ($\Delta 57kb^{homo}$, $0.10H1^{-/-}$, $02H1^{+/-}$; clone name: 17-3-41-25-13), in which 11 out of the 12 histone H1 variant alleles were deleted and only the one 02H1 variant allele was intact (12,13). Since the last *02H1* allele in this cell line could not be deleted by simple homologous gene targeting (13), we developed a different strategy using the 4-hydroxytamoxifen (OHT)-inducible Cre/loxP deletion system to establish completely histone H1-deficient DT40 cells. We first introduced two expression vectors into $H1^{\Delta 11/12}$ cells (Figure 1A); one expressed a Cre-estrogen receptor fusion molecule, Mer-Cre-Mer, and the other contained the C-terminal-eGFP H1R (*H1R-eGFP*) gene flanked by two *loxP* sequences. It has been reported that C-terminal GFP tagging to histone H1 does not affect H1 protein behavior *in vitro* or in living cells (24). Once the transfectant $H1^{\Delta 11/12+flox}$ ($\Delta 57kb^{homo}$, $0.10H1^{-/-}$, $02H1^{+/-}$, *MerCreMer+*, *flox2-H1R-eGFP+*; clone name: 17-3-41-25-13-10) was established, the last *02H1* allele was successfully deleted by homologous recombination, generating a completely endogenous histone H1-null DT40 cell line, $H1^{\Delta 12/12+flox}$ ($\Delta 57kb^{homo}$, $0.10H1^{-/-}$, $02H1^{-/-}$, *MerCreMer+*, *flox2-H1R-eGFP+*; clone name: K11), with a targeting efficiency of 1/215. Southern blot analysis confirmed that the last *02H1* allele was replaced in the *pΔ02H1/Bleo* targeting vector since the ~13-kb HindIII fragment corresponding to the last *02H1* wild-type allele was converted to a ~8.5-kb fragment (*bleomycin* targeted allele) in $H1^{\Delta 12/12+flox}$ cells (Figure 1B and C). Furthermore, Coomassie brilliant blue (CBB) staining of the sodium dodecyl sulfate (SDS)-polyacrylamide gel confirmed the complete absence of endogenous histone H1 protein in $H1^{\Delta 12/12+flox}$ cells (Figure 1D). Endogenous histone H1 proteins separate as two bands: the upper and lower bands correspond to two (H1L and H1R) and four (01H1, 02H1, 03H1, and 0.10H1) variants, respectively (13). Both $H1^{\Delta 11/12}$ and $H1^{\Delta 11/12+flox}$ cells expressed endogenous 02H1 alone, displaying only the lower band. In addition, the ~50-kDa exogenous H1R-eGFP fusion protein was detected in the $H1^{\Delta 11/12+flox}$ cells (Figure 1E). In $H1^{\Delta 12/12+flox}$ cells, the lower 02H1 band was lost, while the H1R-eGFP band remained. $H1^{\Delta 12/12+flox}$ cells were further treated with 4-OHT to delete the exogenous *H1R-eGFP* transgene by Cre/loxP recombination. Five days after OHT treatment, the fluorescence signals of H1R-eGFP were nearly diminished (data not shown). We next subcloned the eGFP-negative clones $H1^{\Delta 12/12}$ #1 and #2 (clone names: K11-5 and K11-7) by a limiting dilution. Both $H1^{\Delta 12/12}$ #1 and #2 cells lost H1R-eGFP expression as well as endogenous histone H1 expression (Figures 1D and E), indicating the establishment of completely histone H1-null mutant DT40 cells.

In chromatin acid extracts, we noticed that the amounts of proteins that migrated slightly faster than H1 increased in H1 mutant DT40 cells, particularly in $H1^{\Delta 12/12+flox}$ and $H1^{\Delta 12/12}$ #1 and #2 cells (Figure 1D, asterisks). These proteins were likely to be high mobility group (HMG) proteins, since histone H1 and HMG protein doses are known to be compensated by each other and they share the same DNA-binding sites (25). Therefore, we determined HMG protein contents in these cells by western blot analysis using anti-HMG1/2 antibody. In total cell lysates, the levels of HMG1/2 were similar among wild-type and H1 mutant cells (Figure 2A), whereas HMG1/2 in Triton-insoluble chromatin fraction was increased in $H1^{\Delta 12/12+flox}$ and $H1^{\Delta 12/12}$ cells (Figure 2B). Thus, in wild-type DT40 cells, the linker DNA appears to be occupied preferentially with H1 even in the presence of a large pool of HMG. When the level of H1 is substantially decreased, or completely depleted, in mutant cells, HMG could become more bound to DNA. However, the amount of chromatin-bound HMG in H1 mutant cells appears still lower than that of H1 in wild-type (Figure 1D), and only a small fraction of HMG was recovered in Triton-insoluble chromatin fraction (Figure 2B). These results suggest that H1 and HMG have different properties and HMG cannot fully compensate for depletion of H1, even though they might have overlapping functions.

Growth defect of H1-null DT40 cells

As histone H1-null mutant DT40 cells could not be obtained from $H1^{\Delta 11/12}$ cells by using a simple gene targeting strategy (13), we speculated that the complete depletion of histone H1 could affect cell growth or survival. The growth rate of $H1^{\Delta 12/12+flox}$ cells was indeed reduced after OHT treatment. After $H1^{\Delta 11/12+flox}$ and $H1^{\Delta 12/12+flox}$ cells were cultured in the presence or absence of OHT for 4 days, treated and untreated cells were mixed in a 10:1 ratio and further cultured. Figure 3A shows the fractions of GFP (H1R-eGFP)-positive cells among the total population at different time points. No enrichment of GFP+ cells among $H1^{\Delta 11/12+flox}$ cells was observed. In contrast, the proportion of GFP+ cells continuously increased in $H1^{\Delta 12/12+flox}$ during the cultivation of the mixed population, suggesting that GFP negative (H1 null) cells grew slowly and were selected out (Figure 3A). However, it should be noted that cell lines missing 11 out of the 12 H1 variants, i.e. $H1^{\Delta 11/12}$, $H1^{\Delta 11/12+flox}$ and $H1^{\Delta 12/12+flox}$, had already shown significant growth defects compared to the wild-type parental cell line (Figure 3B and data not shown), and the complete deletion of H1 further decreased the growth rate. Based on a separate culture experiment, we calculated that the doubling times of wild-type cells, $H1^{\Delta 11/12}$ and $H1^{\Delta 12/12}$ were 9.9 h, 12.6 h and 13.9 h, respectively (Figure 3B, Supplementary Figure S1, and Supplementary Table S1).

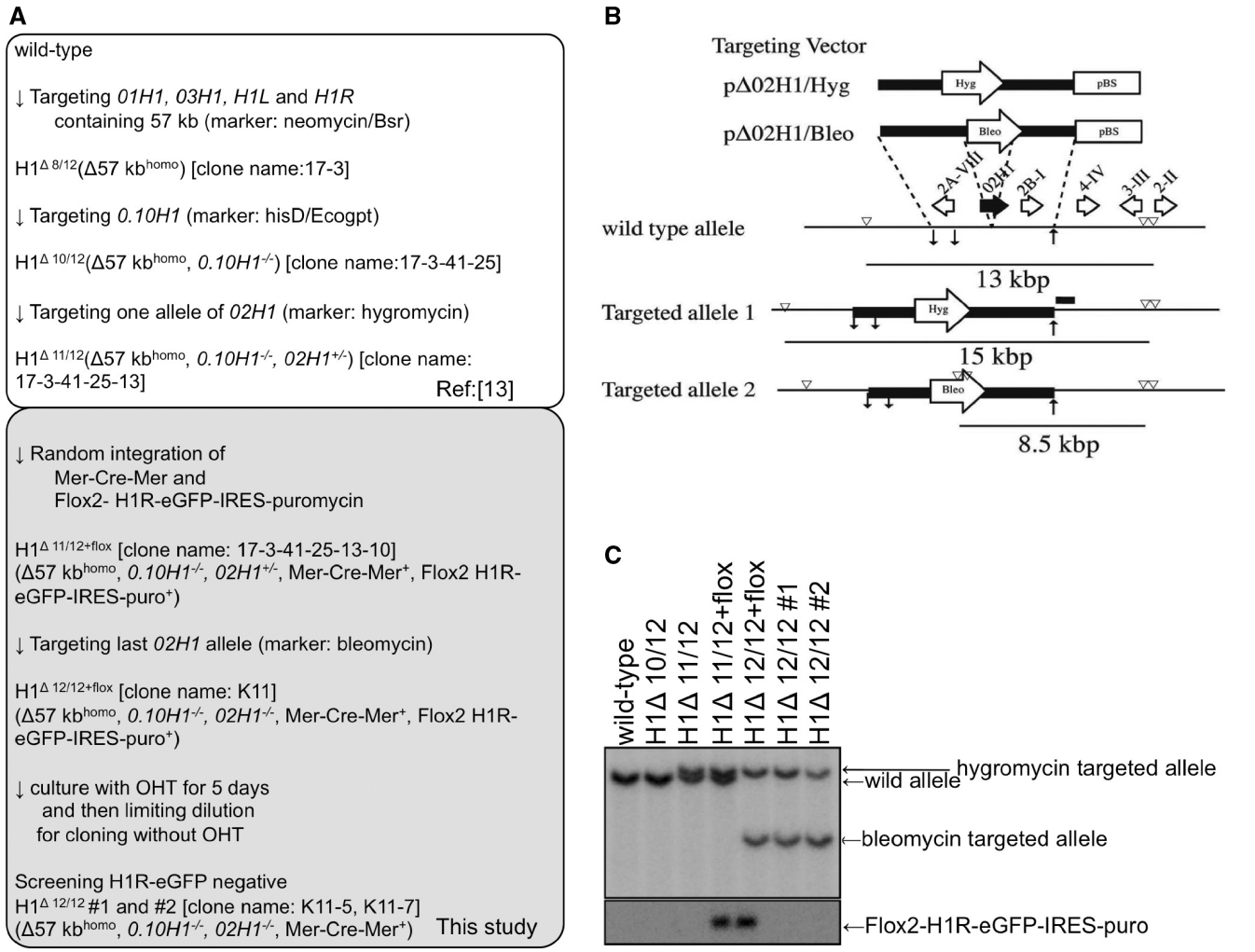

Figure 1. Generation of histone H1-null DT40 cells (**A**) Flow for generating histone H1 null mutant DT40 cells. (**B**) Schematic diagram of the homologous recombination for *02H1* gene disruption. Targeting vectors (*pΔ02H1/hyg* and *pΔ02H1/bleo*) and the wild-type and targeted alleles are indicated with the expected sizes of HindIII-digested fragments. *02H1* and other histone genes are indicated as closed and open arrows, respectively. A bar represents the position of the *02H1-3′* probe for Southern hybridization. (**C**) Southern blot analysis. Genomic DNA was prepared from wild-type, H1$^{\Delta 10/12}$, *H1*$^{\Delta 11/12}$, *H1*$^{\Delta 11/12+flox}$, *H1*$^{\Delta 12/12+flox}$ and *H1*$^{\Delta 12/12}$ #1 and #2 cells, digested with HindIII, and analyzed by Southern blotting using the *02H1-3′1* probe (upper panel) and the eGFP probe (lower panel). (**D**, **E**) Histone H1 proteins are not detected in the H1-null mutant cells. H_2SO_4- and H_2SO_4/$HClO_4$-extracts, which contain all histones and H1, respectively, were prepared from wild-type, *H1*$^{\Delta 10/12}$, *H1*$^{\Delta 11/12}$, *H1*$^{\Delta 11/12+flox}$, *H1*$^{\Delta 12/12+flox}$ and *H1*$^{\Delta 12/12}$ #1 and #2 cells, and separated by 14% SDS-PAGE. Gels were stained with CBB (D) or transferred to a membrane for blotting with anti-GFP to detect H1R-eGFP (E). Asterisks in (D) indicate probable HMG proteins. A representative experiment is shown in all figures.

Global chromatin structure and cell cycle progression are maintained in H1-null DT40 cells

We then examined chromatin structure in histone H1-null mutant cell lines during interphase and mitosis by staining with DAPI. It has been reported that chromosomes are condensed normally in mitotic *Xenopus* egg extract from which H1 has been immunodepleted, whereas extended chromosomes associated with misalignment and missegregation were found in H1-depleted replicated chromatin in different *Xenopus* extracts (26,27). Confocal microscopy analysis revealed that there were no clear morphological differences between wild-type and H1-null (*H1*$^{\Delta 12/12}$) cells, either in condensed mitotic chromosomes (Figure 4A) or in interphase nuclei (Figure 4B). Furthermore, in investigating many paraformaldehyde-fixed mitotic cells and metaphase spreads prepared for chromosome breakage analysis (see below), we found no drastically extended fibers as reported in H1-depleted *Xenopus* cycling extracts (27).

Since H1-null (*H1*$^{\Delta 12/12}$) and most deficient (*H1*$^{\Delta 11/12}$) DT40 cells showed growth defects, we performed a cell cycle analysis by measuring BrdU uptake and DNA content. The distribution of G1, S and G2/M populations was mostly similar between wild-type and *H1*$^{\Delta 12/12}$ cells (Figure 4C). We also monitored the accumulation of cells positive for H3S10ph (an M-phase marker) in the culture after the addition of colcemid (Figure 4D, right). The ratio of H3S10ph-positive cells in steady state (0 h after-colcemid addition) and the accumulation kinetics did

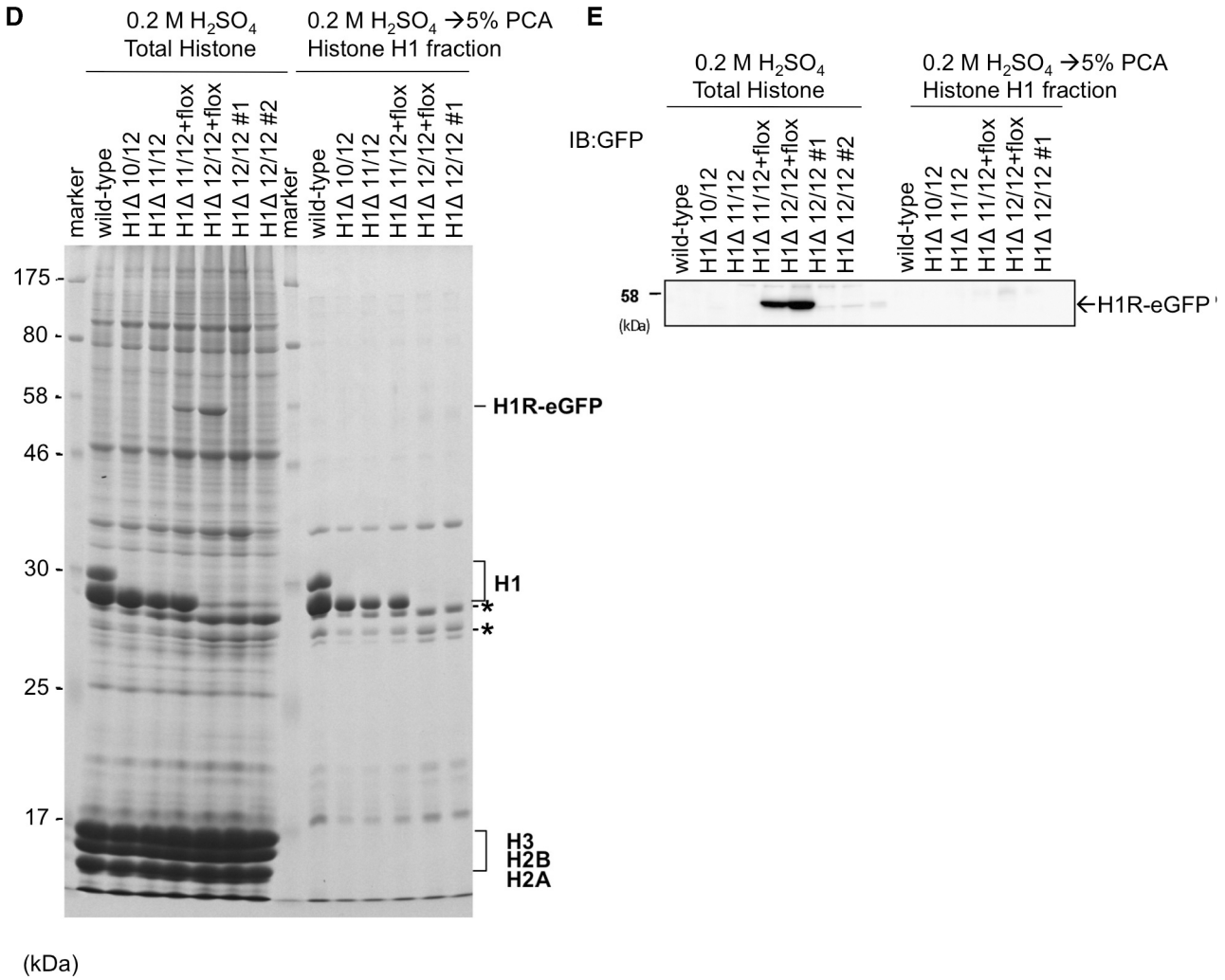

Figure 1. Continued.

not differ between wild-type and $H1^{\Delta 12/12}$ cells (Figure 4D, right). Then, we examined ionizing radiation (IR)-induced G2/M checkpoint activation. After exposing the colcemid-containing culture to 2.3 Gy of IR, the accumulation rate of an H3S10ph-positive population was significantly impaired for 2 h in both wild-type and $H1^{\Delta 12/12}$ cells (Figure 4D, right). In the absence of colcemid, the H3S10ph-positive population was reduced for 2 h in both cell types (Figure 4D, left). Therefore, IR-induced G2/M checkpoint activation appeared to occur in H1-null DT40 cells as it did in wild-type cells. These data suggest that the growth defect in H1-null cells resulted mostly from an extended single cell cycle, but not from a specific cell cycle stage.

Reduction of nucleosome repeat length in H1-mutant DT40 cells

A reduction of ~50% in histone H1 content in mouse *H1c, H1d and H1e* triple KO embryonic stem (ES) cells (0.25 H1 per nucleosome) resulted in a reduction of nucleosome repeat length (NRL) due to micrococcal nuclease (MNase) digestion (4,14). Therefore, we analyzed the NRL for the wild-type, $H1^{\Delta 11/12}$, $H1^{\Delta 11/12+flox}$, $H1^{\Delta 12/12+flox}$ and two histone H1-null mutant cells (Figure 5A and B). Wild-type DT40 cells exhibited an average NRL of ~181 bp. Both $H1^{\Delta 11/12}$ and $H1^{\Delta 11/12+flox}$ cells showed similar lengths with a reduction of ~13 bp: ~167 and ~169 bp, respectively. $H1^{\Delta 12/12+flox}$ and the two H1-null mutant cells, $H1^{\Delta 12/12}$ #1 and #2, displayed an even shorter average NRL: ~163, ~162 and ~163 bp, respectively. These NRL differences seemed to depend on the total amount of histone H1 in a cell. The NRL of $H1^{\Delta 12/12+flox}$ and $H1^{\Delta 12/12}$ mutant cells did not change as much as in the case of the H1-null mutants because the amount of exogenous H1R-eGFP protein was very small compared to the amount of endogenous H1 protein (Figure 1D). The *H1c, H1d* and *H1e* triple KO ES cells have an average NRL of ~174 bp (4,14), and the baseline NRL without histone H1 is predicted to be ~166 bp (28). Therefore, the average NRL calculated in the histone H1-null DT40 cells was mostly

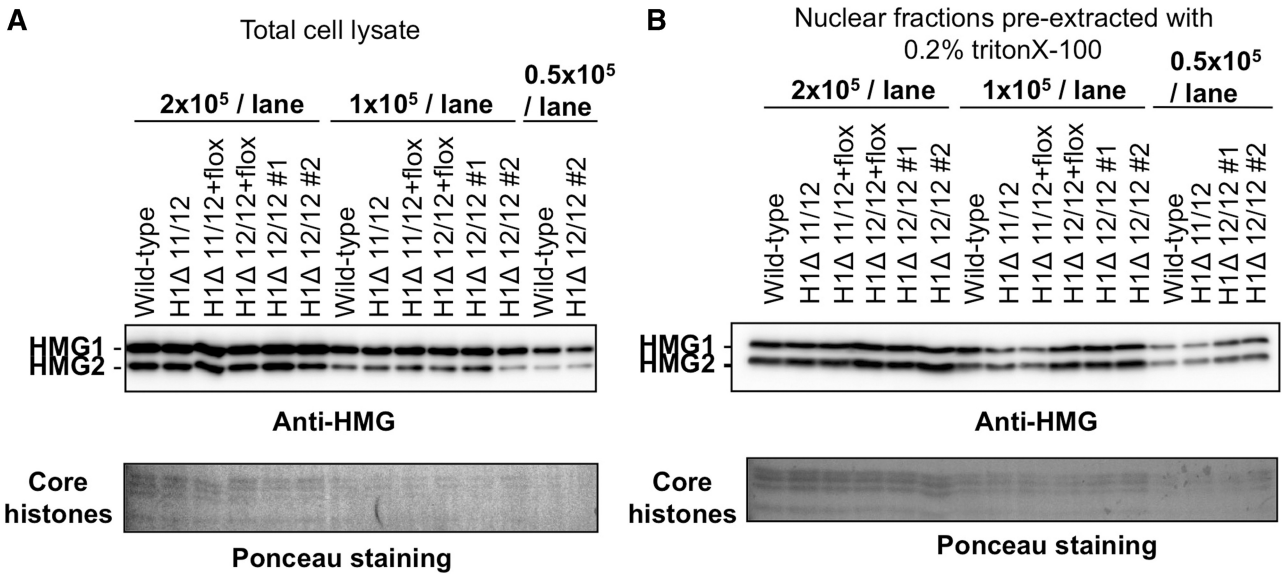

Figure 2. Chromatin bound HMG1/2 is increased in H1-null DT40 cells. Total cell lysate (A) and Triton-insoluble chromatin fraction (B) were separated by 14% SDS-PAGE, blotted onto PVDF membrane, followed by Ponceau S-staining to verify equal protein loading (lower), and then HMG1 and 2 were immunodetected by chemiluminescence (upper).

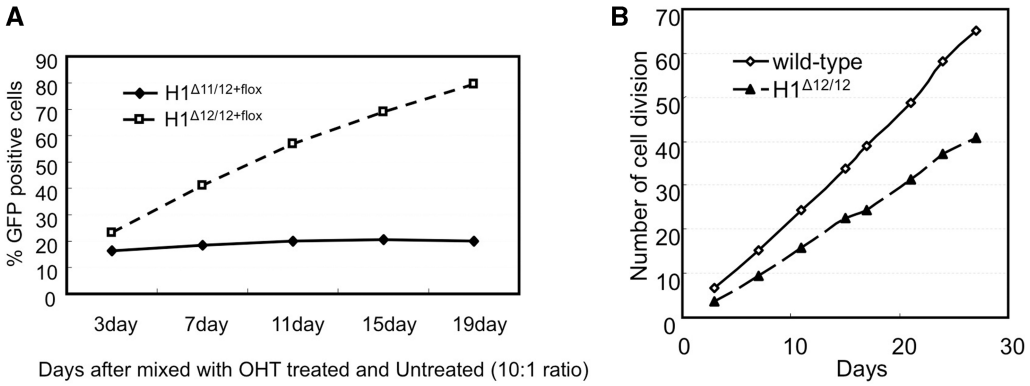

Figure 3. Growth defect of H1-null DT40 cells. (**A**) Slower growth of H1-null cells. Cells harboring H1R-eGFP with or without 02H1 gene ($H1^{\Delta 11/12+flox}$ or $H1^{\Delta 12/12+flox}$) were treated with OHT to remove H1R-eGFP gene, and mixed with OHT-untreated cells with a ratio of 10:1. The percentages of eGFP-positive fractions were monitored using flow cytometry for 19 days. The accumulation rate of GFP positive population in every 4 days from Day 3 to 19 (% average ± SD; $n = 4$) was 0.91 ± 0.97 for $H1^{\Delta 11/12+flox}$ and 14.15 ± 3.19 for $H1^{\Delta 12/12+flox}$. Difference of two values is statistically significant (Student's *t*-test, *P*-value <0.0005). (**B**) Growth curve of wild-type and $H1^{\Delta 12/12+flox}$ cells. The cell division number in every 4 days (average ± SD; $n = 7$) was 9.69 ± 1.34 for wild-type and 6.16 ± 1.11 for $H1^{\Delta 12/12+flox}$. Difference of two values is statistically significant (*P*-value <0.0005).

comparable with the predicted NRL in the total absence of H1.

Linker histone H1 is involved in interphase chromatin compaction

We examined the MNase sensitivity of histone H1-null mutant cells in comparison with wild-type and $H1^{\Delta 11/12}$ cells, but no significant difference was observed (data not shown). Since *Tetrahymena H1*-deficient strains exhibit enlarged nuclei (8), we examined the nuclear volumes of linker histone H1-mutant DT40 cells. Cells were stained with DAPI, and serial z-section images covering the whole nucleus were taken by confocal microscopy. The volume of each nucleus was then calculated using ImageJ software [National Institutes of Health (NIH), Bethesda, MD, USA] (Figure 6). The median nuclear volume (MNV) of wild-type cells was 369.5 μm^3 ($n = 47$). On the contrary, MNV of $H1^{\Delta 11/12}$ and $H1^{\Delta 12/12}$ cells increased by >20%, i.e. 461.9 μm^3 ($n = 27$) and 450 μm^3 ($n = 28$), respectively. These data also suggest that histone H1 is involved in interphase chromatin compaction in chicken DT40 cells.

Increased chromosomal aberrations in histone H1-null mutant DT40 cells

Among the six chicken histone H1 variants, H1R is specifically involved in DNA damage response, and chromosomal instabilities are induced in the *H1R*-deficient DT40 cells (20). Therefore, we compared the rate of

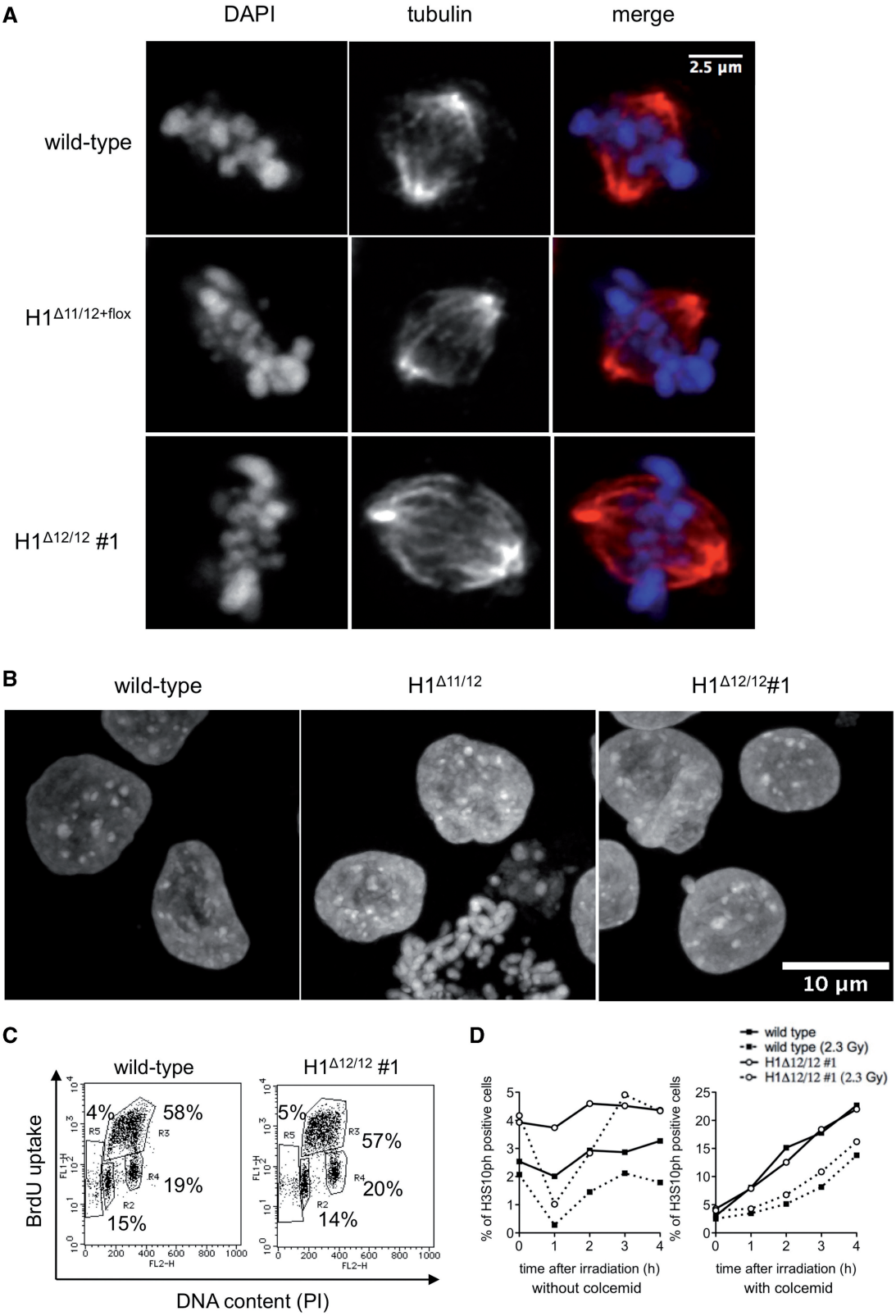

Figure 4. No significant cell cycle defect on histone H1 mutants. (**A**) Mitotic chromosomes in H1 mutant cells. The wild-type and H1 mutant DT40 cells were stained with DAPI (cyan) and anti-α-tubulin followed by Cy3-conjugated anti-mouse IgG (red). Little difference was seen in metaphase chromosomes among the wild-type, $H1^{\Delta 11/12+flox}$ (expressing 02H1 and H1R-eGFP) and $H1^{\Delta 12/12}$ (H1-null) cells. (**B**) Interphase nuclei. Little difference was seen in global structure of interphase nuclei among the wild-type, $H1^{\Delta 11/12}$ (expressing only 02H1) and $H1^{\Delta 12/12}$ (H1-null); however, the nuclear volume was altered (Figure 6). (**C**) Cell-cycle analysis of the wild-type and $H1^{\Delta 12/12}$ (H1-null) cells by flow cytometry. Cells were pulse-labeled with BrdU for 10 min, fixed, and stained with FITC-anti-BrdU to monitor DNA synthesis (vertical axis; log scale) and propidium iodide (PI) to detect DNA content (horizontal axis; linear scale). The cell cycle distributions were similar between two cell types. R2:G1 phase, R3:S phase, R4:G2-M phase, R5: sub-G1 phase. (**D**) Mitotic index of the wild-type and H1-null cells with or without DNA damage. H3S10ph-positive cell fractions in the absence (left) or presence (right) of 0.1 μg/ml colcemid (0–4 h) were monitored by flow cytometry. G2/M checkpoint activation was examined by ionizing radiation (2.3 Gy).

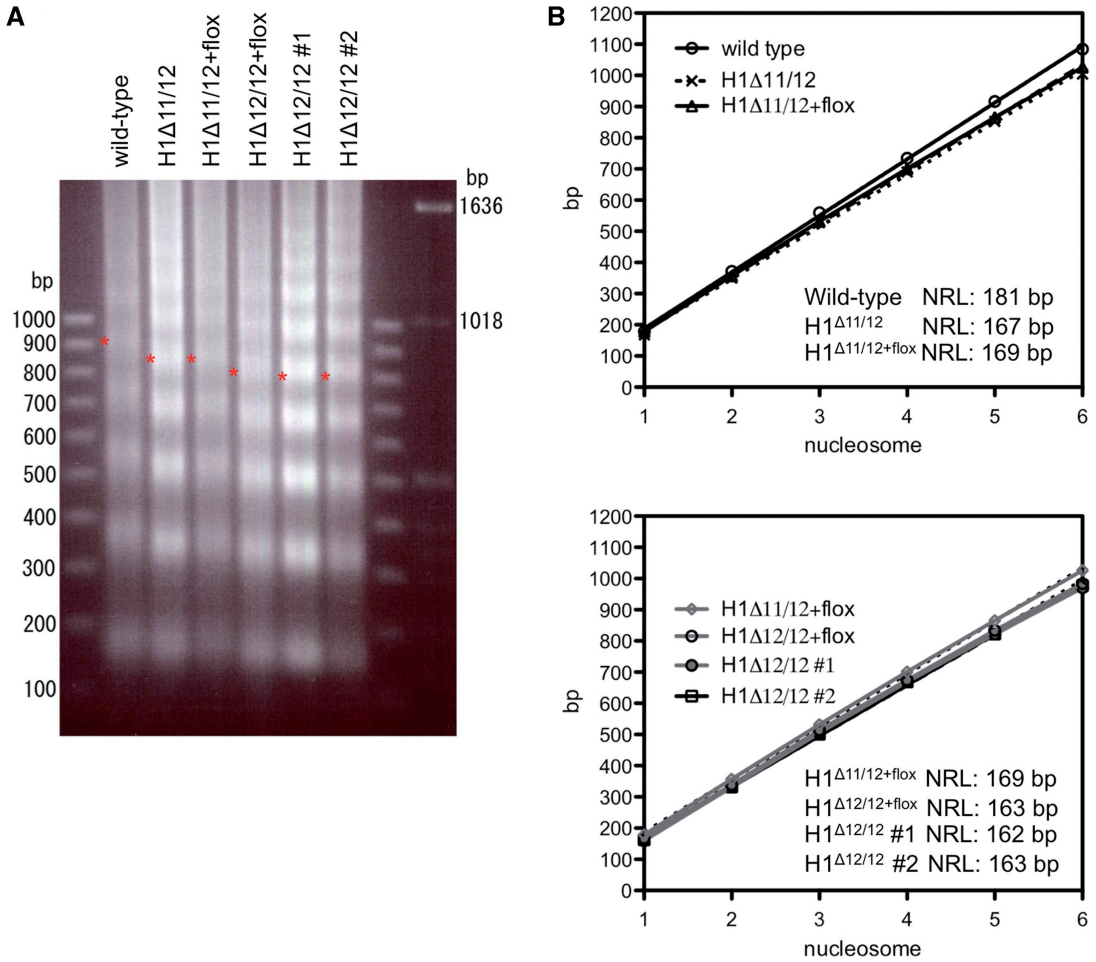

Figure 5. Reduction of NRL in histone H1-null DT40 cells. Nuclei were isolated from DT40 cells and treated with MNase. DNA was then purified, separated on a 1% agarose gel, and stained with ethidium bromide. (**A**) Ethidium-stained agarose gel. Asterisks indicate the position of DNA fragments corresponding to penta-nucleosomes. (**B**) The size of DNA fragment corresponding to each number of nucleosomes was plotted and the NRL was calculated.

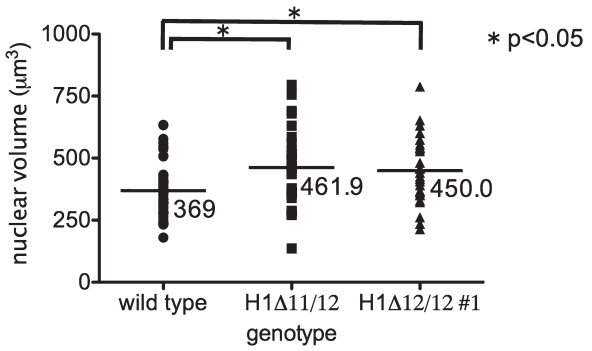

Figure 6. Interphase nuclear volume is increased in H1-null cells. Three-dimensional images of DAPI-stained nuclei were collected using a confocal microscope, and nuclear volumes were measured and plotted. The mean values are indicated. The difference between the wild-type and $H1^{\Delta 11/12}$ or $H1^{\Delta 12/12}$ cells are significant ($P < 0.05$, one-way ANOVA test).

chromosomal aberrations in $H1^{\Delta 12/12}$ #1 and #2 cells with that in wild-type, $H1^{\Delta 11/12}$, $H1^{\Delta 11/12+\mathrm{flox}}$ and $H1^{\Delta 12/12+\mathrm{flox}}$ cells and categorized the chromosomal aberrations according to the International System for Human Cytogenetic Nomenclature (ISCN, 1985) (Table 1 and examples are shown in Supplementary Figure S2). As described previously (20), *H1R*-defective $H1^{\Delta 11/12}$ cells exhibited a high chromosomal aberration rate [0.08 ± 0.014 aberrations per cell (apc) versus 0.02 ± 0.007 apc in wild-type cells] (20). The high chromosomal aberration rate was restored to the wild-type level (0.01 ± 0.004 apc) in $H1^{\Delta 11/12+\mathrm{flox}}$ cells that expressed additional H1R-eGFP. However, $H1^{\Delta 12/12+\mathrm{flox}}$, which expresses only exogenous H1R-eGFP, exhibited higher genomic instability (0.05 ± 0.011 apc) than $H1^{\Delta 11/12+\mathrm{flox}}$. Furthermore, both the histone H1-null mutant cells, $H1^{\Delta 12/12}$ #1 and #2, exhibited the highest chromosomal aberration rates (0.15 ± 0.019 and 0.14 ± 0.025 apc, respectively), which were ~7-fold higher than those of the wild type. Taken together, these results suggest that not only H1R, but also a certain amount of H1 (probably any H1 variant) is crucial for maintenance of chromosomal stability, because (i) histone H1 completely null mutant cells showed the highest chromosomal aberration rate and (ii) $H1^{\Delta 12/12+\mathrm{flox}}$ exhibited a higher chromosomal aberration rate than wild type,

Table 1. Frequency of spontaneous chromosomal aberrations in the wild-type and H1 mutant DT40 cells

Genotype	Isochromatid[a]		Chromatid[a]		Exchange[a]	Aberration (per cell ± S.E.[b])	No. of analyzed Mitotic cells
	Break	Gap	Break	Gap			
Wild type[ref[20]]	0.5	1.5	0.0	0.0	0.0	0.02 ± 0.007	200
$H1^{\Delta 11/12}$	2.0	1.5	1.5	2.0	0.5	0.08 ± 0.014	200
$H1^{\Delta 11/12+flox}$	0.0	0.0	0.0	0.5	0.0	0.01 ± 0.004	200
$H1^{\Delta 12/12+flox}$	1.5	1.0	0.0	1.5	1.0	0.05 ± 0.011	200
$H1^{\Delta 12/12}$ #1	5.0	6.0	2.5	0.5	0.5	0.15 ± 0.019	200
$H1^{\Delta 12/12}$ #2	4.7	2.0	4.0	2.7	0.7	0.14 ± 0.025	150

Cells were treated with colcemid for 1.5 h to enrich mitotic cells.
[a]Data are presented as the number of aberrations per 100 cells.
[b]S.E. is culculated as $x/N \pm \sqrt{x/N}$ (x: total chromosomal aberrations and N: the number of cell.

Table 2. Summary for the affected genes in $H1^{\Delta 12/12+flox}$ and $H1^{\Delta 12/12}$ cells

Expression array analysis among wild-type, $H1^{\Delta 12/12+flox}$ and $H1^{\Delta 12/12}$ cells						
	Wild type versus $H1^{\Delta 12/12+flox}$[a]		Wild type versus $H1^{\Delta 12/12}$[a]		overlap with $H1^{\Delta 12/12+flox}$[a,b]	
>2-fold up	172[c]	(0.3)	215[e]	(2.9)	97	(45.1)
<1/2-fold down	1206[d]	(0.3)	643[f]	(8.6)	363	(58.5)
>4-fold up	44	(0.3)	58	(0.8)	29	(50)
<1/4 fold down	96	(0.3)	115	(1.5)	36	(31.3)
>8-fold up	20	(0.3)	22	(0.3)	16	(72.7)
<1/8-fold down	19	(0.3)	46	(0.6)	12	(26.1)

[a]The number of probes affected in $H1^{\Delta 12/12+flox}$ or $H1^{\Delta 12/12}$ #1 cells in comparison with wild-type cells as base line; values in parenthesis denote % based on the total number of expressed probes 7442 as 100%.
[b]The number of affected probes in $H1^{\Delta 12/12}$ #1 cells which were already affected in $H1^{\Delta 12/12+flox}$ cells in comparison with wild-type cells as base line; values in parenthesis denote % based on the number of affected probes in $H1^{\Delta 12/12}$ #1 cells as 100%.
[c–f]Genelist is provided as Supplementary Table S3–6.

while $H1^{\Delta 11/12+flox}$ or any single *H1* (except *H1R*)-deficient cells did not differ from the wild type (17,20). This markedly high chromosomal aberration rate may be the cause of the growth defect phenotype of the histone H1-deficient cells.

Global impact of H1 depletion on transcription

Another critical issue is whether histone H1 in higher eukaryotes functions as a global transcriptional repressor. Studies of chicken and mouse H1-KO cells suggest that histone H1 is not a global transcriptional repressor; however, a definitive conclusion needs to be made in this regard by using H1-null cells (4,13,17). We performed a gene expression microarray analysis using wild-type cells, $H1^{\Delta 12/12+flox}$, and H1-null mutant $H1^{\Delta 12/12}$ #1 (accession number GSE8483; summarized in Table 2 and Supplementary Table S2). Among the 32 773 target probe sets assayed, 7442 targets (23%) showed significant expression in at least one of the DT40 cell lines analyzed with GeneSpring software (Agilent). The comparison of $H1^{\Delta 12/12+flox}$ cells and wild-type cells revealed that 1378 probes showed changes that were more than 2-fold (172 up and 1206 down; Supplementary Tables S3 and S4 and Supplementary Figure S3). Among these, 44 (0.6%) and 20 (0.3%) were ≥4- and ≥8-fold upregulated, and 96 (1.3%) and 19 (0.3%) were ≥4- and ≥8-fold downregulated, respectively. These data demonstrated that significant reduction in histone H1 content in $H1^{\Delta 12/12+flox}$ cells has a global, but relatively mild, impact on transcription (mostly with less than 4-fold differences). More importantly, most of the changes were due to suppression (87.5%) instead of activation, as would be expected if H1 caused transcriptional repression. Similar changes were observed in the histone H1-null clone $H1^{\Delta 12/12}$ #1 cells, with slightly higher numbers of ≥2-, ≥4- and ≥8-fold upregulated probes, i.e. 215 (2.9%), 58 (0.8%) and 22 (0.3%), respectively (Supplementary Table S5). The number of probes that were downregulated ≥2-, ≥4- and ≥8-fold were 643 (8.6%), 115 (1.5%) and 46 (0.6%), respectively (Supplementary Table S6). Again, 75.9% (643/858) of the probes with more than 2-fold changes in $H1^{\Delta 12/12}$ #1 were downregulated. Notably, ~50% of those affected probes (45.1% and 58.5%) were also up or downregulated in $H1^{\Delta 12/12+flox}$ cells. We confirmed the expression levels of genes in $H1^{\Delta 12/12+flox}$, $H1^{\Delta 12/12}$ #1 and $H1^{\Delta 12/12}$ #2 cells that were up or downregulated by reverse transcriptase-polymerase chain reaction (RT-PCR) analysis (Supplementary Figure S3A). Among the genes that were up or downregulated ≥8-fold in $H1^{\Delta 12/12}$ #1 cells, no clustering toward specific gene families or functions was

detected, and the ontology of the whole probe and that of the ≥8-fold changed genes were quite similar (Supplementary Figure S3B).

These results are consistent with the similar phenotype in H1$^{\Delta 12/12+flox}$ and *H1*$^{\Delta 12/12}$ cells. Even though *H1*$^{\Delta 12/12}$ cells showed more growth defects than *H1*$^{\Delta 12/12+flox}$ cells, this difference was relatively small, and this phenomenon may be because the amount of exogenous H1R-eGFP protein expressed in *H1*$^{\Delta 12/12+flox}$ cells was small compared to that of endogenous H1 expression. It was observed that the NRL of *H1*$^{\Delta 12/12+flox}$ and *H1*$^{\Delta 12/12}$ cells were indistinguishable; therefore, *H1*$^{\Delta 12/12+flox}$ cells may behave like *H1*$^{\Delta 12/12}$ cells in some respects.

DISCUSSION

This report describes the first histone H1 complete KO cells in vertebrates. Our results also indicate that linker histone H1 is not essential for mitotic chromatin condensation and global transcriptional repression in higher eukaryotes, but it does play important roles in nucleosome spacing and interphase nuclear compaction.

Histone H1 and cell growth

Since histone H1-null mutant DT40 cells could not be obtained from *H1*$^{\Delta 11/12}$ cells with a conventional gene targeting strategy (13), we speculated that complete depletion of histone H1 could affect cell growth or survival. Indeed, completely H1-deficient cells, which were successfully generated from conditional lines, displayed growth defects. However, we recently reported that DT40 cells deficient in one of the chicken H1 variants, *H1R,* showed a reduction in homologous gene targeting efficiency (20) and that *02H1*-targeting efficiency in *H1R*-deficient *H1*$^{\Delta 11/12}$ cells was still extremely low (1/215). Using the same targeting vector, wild-type cells were targeted with 3/18 efficiency (data not shown). Therefore, it appears that both the mild growth defect due to complete H1 depletion and the defect in the homologous recombination (HR) pathway of *H1*$^{\Delta 11/12}$ cells probably contributed to the failure to establish completely H1-deficient cells by conventional gene targeting in *H1*$^{\Delta 11/12}$ cells.

A recent report described growth defects in human cell lines caused by single histone H1 variant depletion (18). H1.2 depletion induced the expression of a number of normally repressed cell cycle genes and led to G1-phase arrest, and H1.4 knockdown-induced cell death. *Drosophila* histone H1 knockdown-induced developmental defect and histone H1 triple-KO mice were also embryonic lethal, indicating that histone H1 is essential for development (4,14,19). In chicken DT40 cell lines, we also observed that depletion of multiple H1 variants induced growth defects. However, although H1-null mutant cells are viable, they grow slowly. Thus, histone H1 is not essential for cell growth and survival, at least for the chicken DT40 cell line. However, H1R and completely H1-null mutant cells showed an increased chromosomal aberration rate. Since the p53-mediated cell cycle and DNA damage checkpoint pathway are known to be inactivated in DT40 cells (29), we speculate that complete depletion of histone H1 in cells that have an intact p53 pathway may cause more severely impaired growth phenotypes.

Histone H1, chromatin structure, and genome integrity

Histone H1 (or H1-like protein) integration into chromatin structure and dynamics has been extensively discussed (30–32). So far, experimental data in unicellular organisms has shown that only the micronuclear mitotic chromosome structure is slightly less condensed in the *MLH*-deficient *Tetrahymena* cells (8). In multicellular organisms, normal mitotic chromatin condensation was observed in H1-depleted *Xenopus* egg extracts (27), while defects in chromosome condensation and segregation were seen in replicated chromatin in the absence of H1 in cycling extracts (26). In our experiments as well, histone H1 appeared to be dispensable for mitotic chromatin compaction and segregation in DT40 cells. Nucleosomal architecture was clearly affected by H1 depletion, as shown by the NRL measurements, and the nuclear volume was also increased. While the mechanism by which H1-depletion causes nuclear enlargements remains unknown, the local compaction of polynucleosomes might be affected by electrostatic repulsion of phosphate groups of DNA in the absence of positively charged linker histones. The altered chromatin structure may affect gene expression and chromosomal stability by allowing the access of transcription factors and increasing DNA damage during replication. However, such subtle effects on interphase chromatin might be overwhelmed by strong forces for further chromosome condensation during mitosis, as global metaphase chromatin structure did not appear to be altered in the absence of H1 at the light microscope level. Investigating many mitotic H1-null DT40 cells and chromosome spreads, we never detected drastic morphological changes, similar to extended fibers, seen in H1-depleted *Xenopus* cycling extracts (26). While further higher-resolution and quantitative studies (e.g. by using atomic force microscopy and live cell analysis) will be required to fully evaluate the effect of H1 depletion on mitotic chromosome structure, our data have so far supported earlier work reporting little effect of H1 in *Xenopus* M-phase extract system (27). Alternatively, HMG proteins might compensate for the function of H1 during mitosis, which should also be examined in future.

We also showed that the chromatin aberration rate was increased in H1-null DT40 cells by cytochemical staining of metaphase chromosomes. How is H1 involved in genome integrity? Since the mobility of H1R, but not H1L, in the nucleus decreased after methane methylsulfonate treatment, we speculate that H1R specifically integrates into HR-mediated repair pathways at the chromosome structure level (20). *H1*$^{\Delta 12/12}$ #1 and #2 (H1-null) showed even higher chromosomal aberration rates than that of *H1*$^{\Delta 11/12}$, suggesting that H1 has additional functions besides its involvement in the H1R-mediated pathway for global genome integrity.

Histone H1 and global gene silencing

Transcription of multiple genes was affected in $H1^{\Delta 12/12+flox}$ and $H1^{\Delta 12/12}$ #1 cells. However, the main change was decrease in transcription, suggesting that H1 is involved in transcriptional activation, rather than in global transcriptional repression. Further, individual H1 variant knockdown in human cell lines also suggests that histone H1 generally activates gene expression (18). Further characterization of the established DT40 cells expressing different single H1 variants may clarify the involvement of individual H1 histones in transcriptional regulation.

SUPPLEMENTARY DATA

Supplementary Data are available at NAR Online.

ACKNOWLEDGEMENTS

We thank Xing Zhang and Xiaodong Cheng (Emory University) for critical reading of manuscript, Yoko Hayashi-Takanaka (Osaka University) for technical assistance. Michael Reth (Max-Planck Institute) and Hitoshi Niwa (RIKEN) kindly provided the Mer-Cre-Mer expression vector and the pCAG-IRES-puro expression vector, respectively. We also thank Toshiyuki Matsui (Kyoto University) for the statistical evaluation.

FUNDING

A grant-in-aids from the Ministry of Education, Culture, Sports, Science, and Technology (MEXT) of Japan (to Y.S., Y.T., H.K. and M.T.). Funding for open access charge: MEXT of Japan.

Conflict of interest statement. None declared.

REFERENCES

1. Luger,K., Mader,A.W., Richmond,R.K., Sargent,D.F. and Richmond,T.J. (1997) Crystal structure of the nucleosome core particle at 2.8 A resolution. *Nature*, **389**, 251–260.
2. Davey,C.A., Sargent,D.F., Luger,K., Maeder,A.W. and Richmond,T.J. (2002) Solvent mediated interactions in the structure of the nucleosome core particle at 1.9 a resolution. *J. Mol. Biol.*, **319**, 1097–1113.
3. Ramakrishnan,V., Finch,J.T., Graziano,V., Lee,P.L. and Sweet,R.M. (1993) Crystal structure of globular domain of histone H5 and its implications for nucleosome binding. *Nature*, **362**, 219–223.
4. Fan,Y., Nikitina,T., Zhao,J., Fleury,T.J., Bhattacharyya,R., Bouhassira,E.E., Stein,A., Woodcock,C.L. and Skoultchi,A.I. (2005) Histone H1 depletion in mammals alters global chromatin structure but causes specific changes in gene regulation. *Cell*, **123**, 1199–1212.
5. Thoma,F., Koller,T. and Klug,A. (1979) Involvement of histone H1 in the organization of the nucleosome and of the salt-dependent superstructures of chromatin. *J. Cell. Biol.*, **83**, 403–427.
6. Harvey,A.C. and Downs,J.A. (2004) What functions do linker histones provide? *Mol. Microbiol.*, **53**, 771–775.
7. Shen,X. and Gorovsky,M.A. (1996) Linker histone H1 regulates specific gene expression but not global transcription in vivo. *Cell*, **86**, 475–483.
8. Shen,X., Yu,L., Weir,J.W. and Gorovsky,M.A. (1995) Linker histones are not essential and affect chromatin condensation in vivo. *Cell*, **82**, 47–56.
9. Hellauer,K., Sirard,E. and Turcotte,B. (2001) Decreased expression of specific genes in yeast cells lacking histone H1. *J. Biol. Chem.*, **276**, 13587–13592.
10. Ramon,A., Muro-Pastor,M.I., Scazzocchio,C. and Gonzalez,R. (2000) Deletion of the unique gene encoding a typical histone H1 has no apparent phenotype in Aspergillus nidulans. *Mol. Microbiol.*, **35**, 223–233.
11. Wang,Z., Sirotkin,A., Buchold,G., Skoultchi,A. and Marzluff,W. (1997) The mouse histone H1 genes: gene organization and differential regulation. *J. Mol. Biol.*, **271**, 124–138.
12. Takami,Y., Higashio,M., Fukuoka,T., Takechi,S. and Nakayama,T. (1996) Organization of the chicken histone genes in a major gene cluster and generation of an almost complete set of the core histone protein sequences. *DNA Res.*, **3**, 95–99.
13. Takami,Y. and Nakayama,T. (1997) A single copy of linker H1 genes is enough for proliferation of the DT40 chicken B cell line, and linker H1 variants participate in regulation of gene expression. *Genes Cells*, **2**, 711–723.
14. Fan,Y., Nikitina,T., Morin-Kensicki,E., Zhao,J., Magnuson,T., Woodcock,C. and Skoultchi,A. (2003) H1 linker histones are essential for mouse development and affect nucleosome spacing in vivo. *Mol. Cell. Biol.*, **23**, 4559–4572.
15. Seguchi,K., Takami,Y. and Nakayama,T. (1995) Targeted disruption of 01H1 encoding a particular H1 histone variant causes changes in protein patterns in the DT40 chicken B cell line. *J. Mol. Biol.*, **254**, 869–880.
16. Takami,Y. and Nakayama,T. (1997) One allele of the major histone gene cluster is enough for cell proliferation of the DT40 chicken B cell line. *Biochim. Biophys. Acta*, **1354**, 105–115.
17. Takami,Y., Nishi,R. and Nakayama,T. (2000) Histone H1 variants play individual roles in transcription regulation in the DT40 chicken B cell line. *Biochem. Biophys. Res. Commun.*, **268**, 501–508.
18. Sancho,M., Diani,E., Beato,M. and Jordan,A. (2008) Depletion of human histone H1 variants uncovers specific roles in gene expression and cell growth. *PLoS Genet.*, **4**, e1000227.
19. Lu,X., Wontakal,S.N., Emelyanov,A.V., Morcillo,P., Konev,A.Y., Fyodorov,D.V. and Skoultchi,A.I. (2009) Linker histone H1 is essential for Drosophila development, the establishment of pericentric heterochromatin, and a normal polytene chromosome structure. *Genes Dev.*, **23**, 452–465.
20. Hashimoto,H., Sonoda,E., Takami,Y., Kimura,H., Nakayama,T., Tachibana,M., Takeda,S. and Shinkai,Y. (2007) Histone H1 variant, H1R is involved in DNA damage response. *DNA Repair*, **6**, 1584–1595.
21. Sonoda,E., Sasaki,M., Buerstedde,J., Bezzubova,O., Shinohara,A., Ogawa,H., Takata,M., Yamaguchi-Iwai,Y. and Takeda,S. (1998) Rad51-deficient vertebrate cells accumulate chromosomal breaks prior to cell death. *EMBO J.*, **17**, 598–608.
22. van Holde,K.E. (1989) *Chromatin*. Springer-Verlag, New York.
23. Ito,I., Mitsuoka,N., Sobajima,J., Uesugi,H., Ozaki,S., Ohya,K. and Yoshida,M. (2004) Conformational difference in HMGB1 proteins of human neutrophils and lymphocytes revealed by epitope mapping of a monoclonal antibody. *J. Biochem.*, **136**, 155–162.
24. Misteli,T., Gunjan,A., Hock,R., Bustin,M. and Brown,D.T. (2000) Dynamic binding of histone H1 to chromatin in living cells. *Nature*, **408**, 877–881.
25. Catez,F., Brown,D.T., Misteli,T. and Bustin,M. (2002) Competition between histone H1 and HMGN proteins for chromatin binding sites. *EMBO Rep.*, **3**, 760–766.
26. Maresca,T.J., Freedman,B.S. and Heald,R. (2005) Histone H1 is essential for mitotic chromosome architecture and segregation in Xenopus laevis egg extracts. *J. Cell. Biol.*, **169**, 859–869.

27. Ohsumi,K., Katagiri,C. and Kishimoto,T. (1993) Chromosome condensation in Xenopus mitotic extracts without histone H1. *Science*, **262**, 2033–2035.
28. Woodcock,C.L., Skoultchi,A.I. and Fan,Y. (2006) Role of linker histone in chromatin structure and function: H1 stoichiometry and nucleosome repeat length. *Chromosome Res.*, **14**, 17–25.
29. Ulrich,E., Boehmelt,G., Bird,A. and Beug,H. (1992) Immortalization of conditionally transformed chicken cells: loss of normal p53 expression is an early step that is independent of cell transformation. *Genes Dev.*, **6**, 876–887.
30. Bustin,M., Catez,F. and Lim,J.H. (2005) The dynamics of histone H1 function in chromatin. *Mol. Cell*, **17**, 617–620.
31. Thomas,J.O. (1999) Histone H1: location and role. *Curr. Opin. Cell. Biol.*, **11**, 312–317.
32. Wolffe,A.P., Khochbin,S. and Dimitrov,S. (1997) What do linker histones do in chromatin? *Bioessays*, **19**, 249–255.